Geophysical Research Letters

RESEARCH LETTER
10.1029/2022GL099808

Key Points:

- Mean bedform trough depths and set thickness show a parabolic dependence on transport stage peaking under mixed-load transport conditions
- Mean set thickness is a poor indicator of flow depth, but depth-normalized mean set thickness is strongly influenced by transport stage
- Transport stage exerts a key control on preserved fluvial strata and should be considered in paleo-hydraulic reconstructions

Supporting Information:

Supporting Information may be found in the online version of this article.

Correspondence to:

D. Das,
debsmita.das@geog.ucsb.edu

Citation:

Das, D., Ganti, V., Bradley, R., Venditti, J., Reesink, A., & Parsons, D. R. (2022). The influence of transport stage on preserved fluvial cross strata. *Geophysical Research Letters*, *49*, e2022GL099808. https://doi.org/10.1029/2022GL099808

Received 1 JUN 2022
Accepted 13 SEP 2022

Author Contributions:

Conceptualization: Debsmita Das, Vamsi Ganti
Data curation: Ryan Bradley, Jeremy Venditti
Formal analysis: Debsmita Das, Vamsi Ganti
Funding acquisition: Vamsi Ganti
Investigation: Debsmita Das, Vamsi Ganti
Methodology: Debsmita Das, Vamsi Ganti, Ryan Bradley, Jeremy Venditti
Project Administration: Vamsi Ganti
Supervision: Vamsi Ganti
Writing – original draft: Debsmita Das, Vamsi Ganti
Writing – review & editing: Debsmita Das, Vamsi Ganti, Ryan Bradley, Jeremy Venditti, Arjan Reesink

The Influence of Transport Stage on Preserved Fluvial Cross Strata

Debsmita Das[1], Vamsi Ganti[1,2], Ryan Bradley[3,4], Jeremy Venditti[3,5], Arjan Reesink[6,7], and Daniel R. Parsons[8]

[1]Department of Geography, University of California Santa Barbara, Santa Barbara, CA, USA, [2]Department of Earth Science, University of California Santa Barbara, Santa Barbara, CA, USA, [3]School of Environmental Science, Simon Fraser University, Burnaby, BC, Canada, [4]Northwest Hydraulic Consultants, North Vancouver, BC, Canada, [5]Department of Geography, Simon Fraser University, Burnaby, BC, Canada, [6]Energy and Environmental Institute, University of Hull, Hull, UK, [7]Lancing College, Lancing, UK, [8]Geography and Environment, Loughborough University, Leicestershire, UK

Abstract Fluvial cross strata are depositional products of bedform migration that record formative flow and sediment transport conditions on planetary bodies. Bedform evolution varies with transport stage even under constant flow depths, but our understanding of how prevailing sediment transport conditions affect preserved cross strata is limited. Here, we analyzed experimental bedform evolution and preserved set thickness spanning threshold-of-motion to suspension-dominated transport conditions at multiple equilibrium flow depths. Results show that bedform trough depth and mean preserved set thickness have a parabolic dependence on transport stage, with maximum values observed at intermediate transport stages. Our results indicate that transport stage is a key control on the flow-depth-normalized set thickness but set thickness is a poor indicator of flow depth. Thus, the dependence of bedform dimensions on transport stage should be considered in paleohydraulic reconstruction, and the analysis of set thickness may aid in the estimation of ancient fluvial sediment flux.

Plain Language Summary Alluvial rivers have ripples and dunes (i.e., bedforms) that migrate across the riverbed, resulting in characteristic signatures called cross strata found in river deposits on Earth and Mars. Cross strata encode information about the flow and sediment transport conditions under which bedforms evolved. For over a century, the relation between cross strata thickness and formative flow conditions has been studied. However, we do not understand how prevailing sediment transport conditions control set thickness distributions. We used high-resolution topography of bedform evolution from controlled physical experiments where transport stage—a parameter that quantifies sediment transport intensity—was systematically changed across multiple flow depths. We discovered that preserved cross set thickness is primarily controlled by transport stage, and that the mean set thickness of preserved deposits is a poor indicator of flow depth. We develop a new mathematical function that describes the dependence of mean set thickness on the formative transport stage. Our work indicates that the transport-stage dependence of set thickness should be a primary consideration in paleohydraulic reconstruction, and that analysis of cross strata may aid the estimation of paleo-sediment-transport conditions.

1. Introduction

The migration of bedforms (e.g., ripples, dunes, and bars) on riverbeds results in the deposition of cross-stratified sedimentary structures or cross sets (Allen, 1963a, 1963b; Allen, 1970, 1982; Rubin & Hunter, 1982; Sorby, 1859). Fluvial cross strata are ubiquitous features on Earth and Mars (Best & Fielding, 2019; Edgar et al., 2018), and they record formative flow and sediment transport conditions (Allen, 1970; Jerolmack & Mohrig, 2005; Mahon & McElroy, 2018; Yalin, 1964). Therefore, the quantitative interpretation of fluvial cross strata is an integral part of the paleohydraulic reconstruction toolkit (e.g., Bhattacharya & Tye, 2004; Bridge & Tye, 2000; Ganti et al., 2019). Existing research describes how preserved cross strata record formative flow characteristics under steady and unsteady conditions (e.g., Ganti et al., 2013; Jerolmack & Mohrig, 2005; Leary & Ganti, 2020; Leclair, 2002; Leclair & Bridge, 2001; Paola & Borgman, 1991). However, our understanding of how prevailing sediment transport conditions affect fluvial cross strata remains limited. A mechanistic understanding of how sediment transport influences bedform geometry, kinematics and resulting deposits is needed to improve inferences of paleo-sediment transport rates from ancient fluvial facies.

Fluvial cross strata are comprised of cross-stratified layers bounded by erosional surfaces. The erosional surfaces are a consequence of a migrating train of bedforms, whereby troughs of migrating bedforms erode some fraction of the downstream bedform deposits (e.g., Paola & Borgman, 1991). The formation of cross strata is therefore dependent on trough depth variability and bed aggradation rates—parameters that determine the susceptibility of deposits to erosion and later reworking (Allen, 1970, 1973; Jerolmack & Mohrig, 2005; Paola & Borgman, 1991; Rubin, 1987; Sorby, 1859). Over a century of research has led to scaling relations between preserved set geometry (parametrized by thickness between successive erosional boundaries, D_{st}) and the dimensions and kinematics of bedforms under steady flows (Ganti et al., 2013; Leclair, 2002; McElroy & Mohrig, 2009; Paola & Borgman, 1991). Paola and Borgman (1991) formulated the variability-dominated model of set preservation which, under minimal net aggradation, relates set thickness distribution to the gamma-distributed formative bedform heights. This approach was thereafter modified to account for low bedform climb angles and to derive predictive models for quantifying bedform heights from cross-set thickness (Bridge, 2003; Bridge & Best, 1997; Leclair & Bridge, 2001; Leclair et al., 1997; Storms et al., 1999). Together, experiments and theory indicate that mean formative bedform heights are 2.9 ± 0.7 times the mean set thickness under low net aggradation rates. Moreover, the variability-dominated preservation model predicts that the coefficient of variation of the preserved set thickness (CV (D_{st})) is a near-constant value of 0.88—a condition often observed in steady-state experiments but seldom observed in outcrops (Lyster et al., 2022). Numerical, experimental, and field studies show that preservation ratio of bedforms, the ratio of the mean D_{st} and mean bedform heights, and CV (D_{st}) can change due to flow variability and the coevolution of river dunes and bars—scenarios characterized by high localized angles of bedform climb (Reesink et al., 2015; Ganti et al., 2020; Leary & Ganti, 2020; Paola et al., 2018).

Despite insights into how prevailing flow affects cross-stratal preservation, it is unclear how sediment-transport conditions change set preservation. Interpreting this connection requires a two-stage approach that includes characterizing the influence of transport conditions on bedform morphology and kinematics, and linking these parameters to cross-stratal geometry. Experimental and field observations demonstrate that equilibrium bedform geometry can vary significantly with transport stage—the ratio of the Shields stress (τ^*) to the critical Shields stress (τ_c^*)—for a given flow depth (Allen, 1982; Bradley and Venditti, 2017, 2021; Venditti et al., 2016). Bedform height is a parabolic function of transport stage for a given flow depth, where maximum equilibrium bedform heights occur at intermediate transport stages (e.g., R. W. Bradley and Venditti, 2019b). The dependence of bedform heights on transport stage was documented in natural rivers during floods, where transport stage variations during a flood hydrograph led to the adjustment of bedform sizes, accompanied by complex patterns of hysteresis (Hu et al., 2021; R. W. Bradley and Venditti, 2021). The transport stage effect on bedform evolution should impact preserved cross strata because set preservation is driven by trough scour depth variability and local bedform climb angle (Bridge & Best, 1997; Paola & Borgman, 1991). Here, we analyzed a series of controlled physical experiments of steady-state bedform evolution to uncover how transport stage affects set preservation.

2. Material and Methods

2.1. Experimental Setup and Data Collection

We analyzed 12 steady-state experiments of bedform evolution conducted in a 15 m long, 1 m wide, and 0.6 m deep flume at the River Dynamics Laboratory at Simon Fraser University (Bradley and Venditti, 2019a, 2019b; R. Bradley, 2018). The experiments were conducted using medium-to-coarse sand (median grain size, $D_{50} = 0.55$ mm) under subcritical flow conditions. Of the 12 experiments, five experiments each had an initial flow depth (h) of 0.15 and 0.20 m, and two experiments had $h = 0.25$ m. For each flow depth, water discharge and flume slope were systematically varied to change the dominant mode of sediment transport from threshold-of-motion (THLD) to bedload-dominated (BDLD) to mixed-load (lower and upper: LMIX/UMIX) to suspension-dominated (SPSN) conditions. For the experiments with $h = 0.25$ m, only THLD and BDLD experiments were performed. The equilibrium water surface slope ranged from 0.0008 for THLD conditions to 0.005 for SPSN conditions. Experiments were conducted with constant sediment and water discharge for 10–25 hr prior to data collection, which allowed the flow depth, water surface slope and bedform dimensions to equilibrate with prevailing conditions (R. W. Bradley and Venditti, 2019b).

Bed elevation evolution data were collected using a swath mapping system comprising 32 ultrasound scanners between 4.5 and 10 m in the downstream direction to eliminate entrance and exit effects. The cross-stream and downstream spacing between data points are 25 and 12.9 mm, respectively, and the temporal resolution of

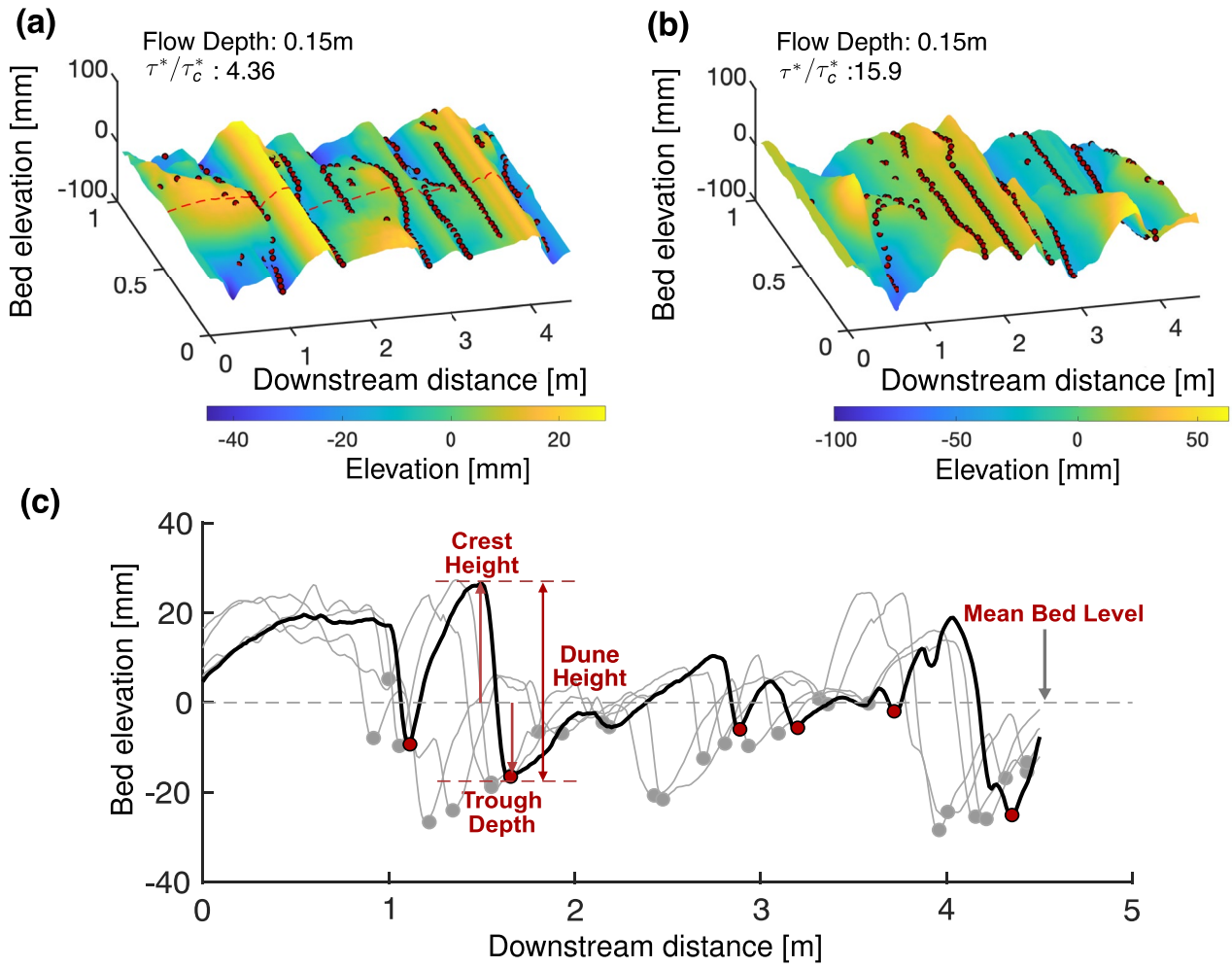

Figure 1. Bed elevation scans from the (a) threshold-dominated and (b) lower-mixed-load transport conditions at flow depth of 0.15 m. Red markers denote the bedform troughs identified using Lee et al. (2021). (c) Example detrended bed elevation profile from (a) (red dashed line), where the mean bed level, crest height, bedform height, and trough depth are highlighted. The gray lines indicate the same profile at earlier time steps, highlighting migration of trough scours.

the data is 10 min. Bed elevation evolution data were collected over a 10 hr duration, and R. W. Bradley and Venditti (2019b) reported that a statistical steady-state, based on bedform dimensions, was achieved in all experiments for the last six hours of this observational window. We, therefore, restricted our analysis to the last five hours of this six-hour-window, which comprised 30 topographic scans.

2.2. Quantifying Bedform Dimensions and Kinematics

We used the bedform tracking tool of Lee et al. (2021) to quantify the geometry and kinematics of bedform evolution (Text S1 in Supporting Information S1). Lee et al. (2021) identify bedform troughs and crests from the change in sign of the gradient of the bed profile where a positive or a negative change in the gradient indicates a trough or a crest, respectively. We analyzed 32 longitudinal profiles for each experiment and validated the estimated bedform heights (H) and lengths (L) with those reported in R. W. Bradley and Venditti (2019b) (Figure S1 in Supporting Information S1). We also quantified the bedform migration rates to assess the typical migration timescale: the ratio of mean bedform length and mean bedform celerity.

We estimated the trough depths (H_t)—the parameter that leads to generation of set boundaries (Paola & Borgman, 1991)—as the vertical distance between a bedform trough and the mean elevation of the detrended bed elevation profile (Figure 1c). We compared the empirical distribution of H_t with a two-parameter Gamma distribution,

$$f(H_t) = \frac{H_t^{\alpha-1} \exp(-H_t/\beta)}{\beta^{\alpha} T(\alpha)} \quad (1)$$

where α and β are the shape and scale parameter, respectively. We computed the statistics of bedform dimensions and kinematic rates by averaging them over time and also across the 32 longitudinal profiles. We denote the spatial and temporal averaging using the overbar ($\bar{\cdot}$) and angled brackets ($\langle . \rangle$), respectively.

Finally, following Bradley and Venditti (2019a), we used transport stage (τ^*/τ_c^*) as indicator of sediment transport conditions, where the Shields stress is (Shields, 1936):

$$\tau^* = \frac{\tau}{(\rho_s - \rho_w) g D_{50}} \quad (2)$$

in which τ is the bed shear stress, ρ_s and ρ_w are the densities of sediment and water, respectively, and g is the acceleration due to gravity. For all experiments, $\tau_c^* = 0.03$ (R. W. Bradley and Venditti, 2019b). Transport stage varied from 4.36 to 25.61 across the experiments, and the minimum and maximum τ^*/τ_c^* values corresponded with the THLD experiment with $h = 0.15$ m and the SPSN experiment with $h = 0.20$ m, respectively. For 0.15, 0.20, and 0.25 m flow depths, τ^*/τ_c^* varied from 4.36 to 23.5, 5.5 to 26.5, and 9 to 13.5, respectively.

2.3. Quantifying the Geometry of Fluvial Strata

For each experiment, we generated synthetic stratigraphic sections by stacking time series of bed elevation profiles and clipping eroded parts of topography (Ganti et al., 2013). The synthetic stratigraphy constitutes both sampled topography (i.e., partially preserved lee faces) and erosional set boundaries that were constructed in the course of bedform trough migration (cf. Ganti et al., 2013). To delineate the constructed set boundaries from sampled topography, we retained surfaces that were a migration timescale apart from each other starting with the oldest surface and skipped every surface below this temporal resolution (Ganti et al., 2013). We excluded the latest topographic surface for set thickness computation. We measured D_{st} as the vertical sedimentary thickness that is bounded by successive erosional boundaries. We compared the empirical distribution of D_{st} with the theoretical expectation of the variability-dominated preservation model, given by:

$$f(D_{st}) = \frac{a e^{-aD_{st}} \left(e^{-aD_{st}} + a^{D_{st}} - 1\right)}{(1 - e^{-aD_{st}})^2} \quad (3)$$

where a is the exponential tail parameter. The theory of Paola and Borgman (1991) indicates that the parameter a is related to the scale parameter of the trough-depth distribution (Equation 1) as $\beta = 1/a$.

Finally, we computed the preservation ratio for each longitudinal profile in the cross-stream direction, ω, and the experiment, $\langle\omega\rangle$, as $\overline{D_{st}}/\overline{H}$ and $\left\langle \overline{D_{st}} \right\rangle / \left\langle \overline{H} \right\rangle$, respectively. We also computed $CV(D_{st})$ for each longitudinal profile of each experiment.

3. Results

3.1. Transport Stage Controls Bedform Geometry and Trough Depth

The bedform dimensions calculated from the method of Lee et al. (2021) follow the same patterns documented in R. W. Bradley and Venditti (2019b). The bedform heights displayed a parabolic relation with transport stage (Figure 2a), where $\left\langle \overline{H} \right\rangle$ ranged from 0.026 ± 0.0043 m (mean ± S.D.) for $\frac{\tau^*}{\tau_c^*} = 4.36$ ($h = 0.15$ m) to a peak value of 0.061 ± 0.008 m for $\frac{\tau^*}{\tau_c^*} = 15.69$ ($h = 0.20$ m). The bedform heights diminished beyond this τ^*/τ_c^* value with $\left\langle \overline{H} \right\rangle = 0.044 \pm 0.014$ m for $\frac{\tau^*}{\tau_c^*} = 26.5$($h = 0.20$ m). The bedform lengths (L) remained relatively consistent at lower transport stages (THLD, BDLD, LMIX) and increased for higher transport stages.

Similar to the bedform heights, trough scour depths are controlled by transport stage (Figure 2b). Data show that for all flow depths, low transport stages are associated with shallow trough scour depths (Figures 2a and 2b). With increasing transport stage, trough depths became progressively deeper, reaching a maximum value under bedload-dominated and lower-mixed-load transport conditions (Figure 2b). At even higher transport stages (UMIX

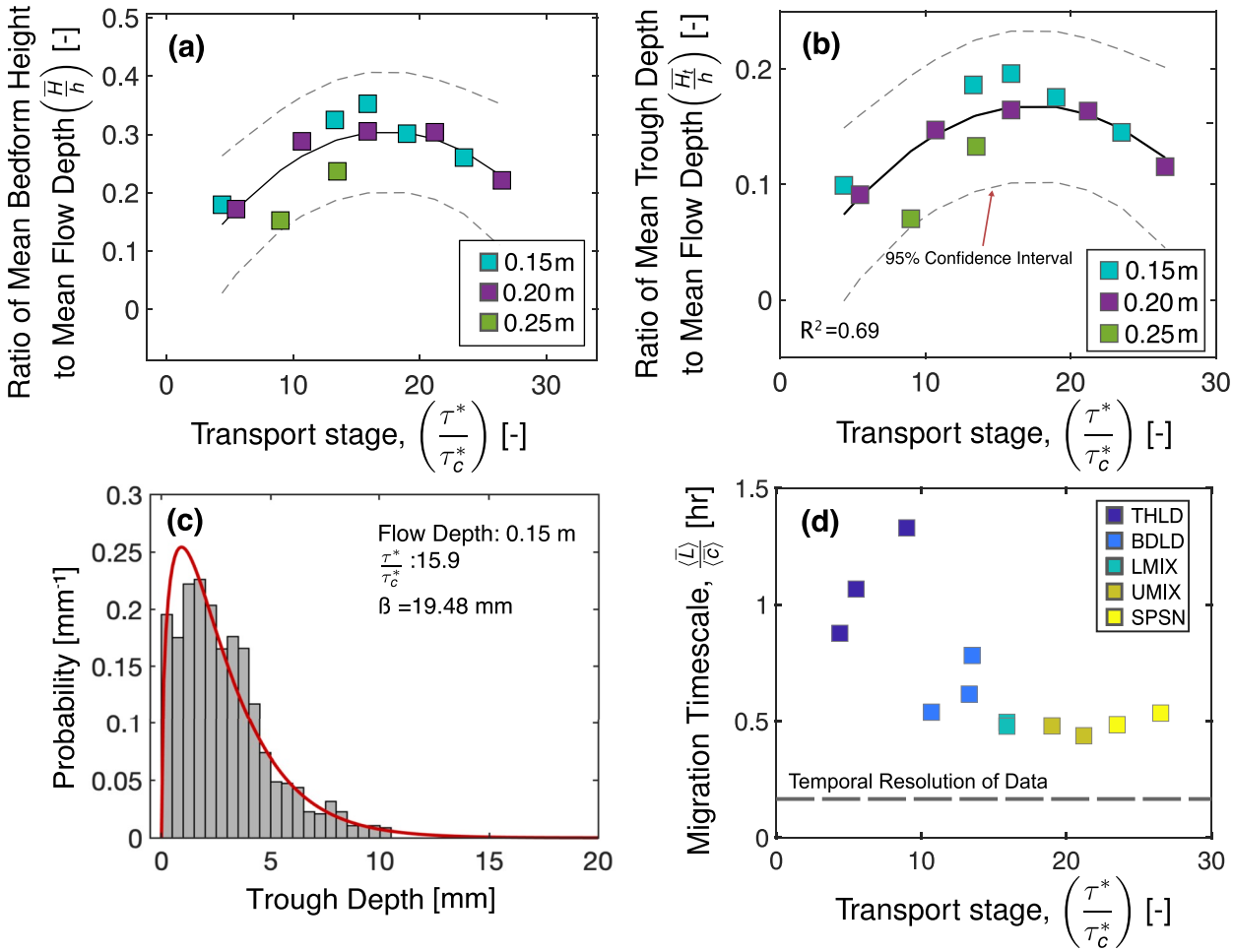

Figure 2. The functional dependence of flow-depth-normalized (a) mean bedform height and (b) mean trough depth on transport stage. The solid and dashed lines indicate the best-fitting parabolic function and its 95% confidence intervals. (c) Probability density function of trough scour depths for mixed-load transport conditions at flow depth of 0.15 m. Gray bars and red line indicate the empirical density and the best-fitting Gamma distribution, respectively (Equation 1). (d) Estimated migration timescale as a function of transport stage, with the dashed line indicating the temporal resolution of bed evolution data.

and SPSN conditions), the volume of suspended sediment increased resulting in the elongation of bedforms and shallowing of troughs until the wash out of dunes occurred (R. W. Bradley and Venditti, 2019b). We also found that $\left\langle \overline{H_t} \right\rangle$ was larger at higher h for every transport stage (Figure 2b), and a two-parameter Gamma distribution adequately described H_t in all experiments (Figures 2c and S2 in Supporting Information S1). The scale parameter of the trough-depth distribution (Equation 1) increased from 0.0908 m^{-1} to 1.8763 m^{-1} for threshold-of-motion to suspension-dominated transport conditions. Finally, the flow-depth normalized $\left\langle \overline{H_t} \right\rangle$ displayed a parabolic dependence on transport stage ($R^2 = 0.69$) peaking under bedload-dominated and lower-mixed-load conditions (Figure 2b).

Bedform migration rates (c) increased with transport stage from threshold-of-motion to intermediate transport stage conditions at all flow depths. For $h = 0.15$ m, $\left\langle \overline{c} \right\rangle$ increased from ~0.2 mm/s at THLD to ~0.55 mm/s at UMIX stage (Figure S3 in Supporting Information S1). At even higher transport stages, $\left\langle \overline{c} \right\rangle$remained relatively constant (Figure S3 in Supporting Information S1). The translation timescales, computed as $\left\langle \overline{L} \right\rangle / \left\langle \overline{c} \right\rangle$, ranged from 1.2 hr for THLD to 15 min for SPSN experiments (Figure 2d).

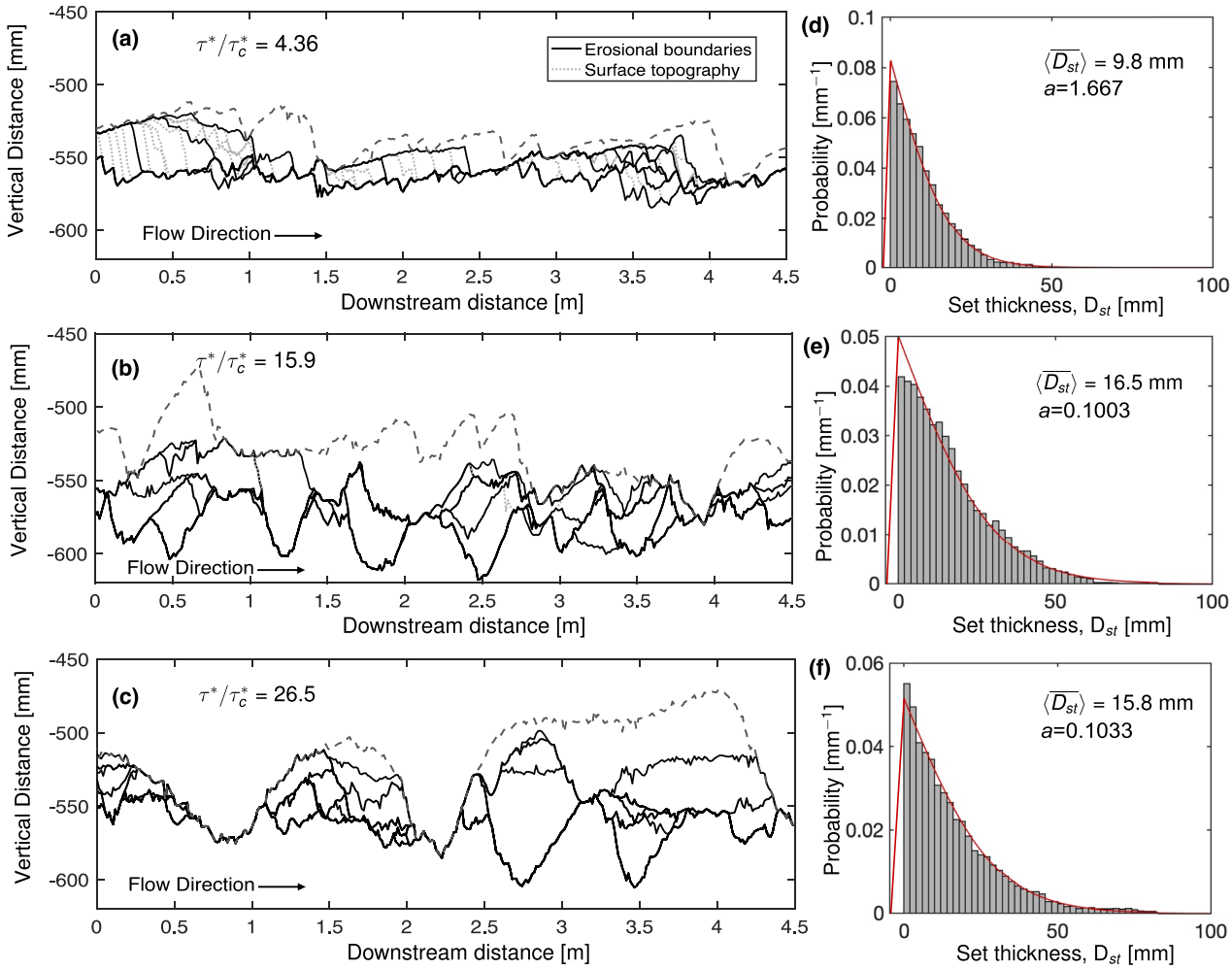

Figure 3. Example synthetic stratigraphic sections built from bed evolution data in the depositional-dip direction for a flow depth of 0.15 m under (a) threshold-dominated, (b) lower-mixed-load, and (c) upper-mixed-load transport conditions. The dashed black line shows the final topography not considered in computation of set thickness, and the gray dashed lines indicate the filtered lee faces of bedforms. Solid lines indicate erosional boundaries. Panels (d–f) show empirical probability density functions of measured set thickness (gray bars) and the best-fitting distribution expected under the variability-dominated preservation model (red line; Equation 3).

3.2. Transport Stage Controls Preserved Set Thickness

The preserved set thickness varied systematically with transport stage (Figures 3a–3c). Our results showed that $\left\langle \overline{D_{st}} \right\rangle$ with h = 0.15 m increased from 0.010 ± 0.0016 m (mean ± S.D.) to 0.021 ± 0.0034 m for THLD and BDLD experiments, respectively. The value fell to 0.016 ± 0.0032 m for the SPSN experiment. We observed a similar trend for the preserved set thickness with h = 0.20 m, for which peak $\left\langle \overline{D_{st}} \right\rangle$ values corresponded with the lower-mixed-load transport conditions. In contrast, there was no significant trend between $\left\langle \overline{D_{st}} \right\rangle$ and h (Figure 4a). The $\left\langle \overline{D_{st}} \right\rangle$ value ranged from 0.01 to 0.021 m for h = 0.15 and 0.012 m–0.02 m for h = 0.20 m.

Our results revealed that the flow-depth-normalized $\left\langle \overline{D_{st}} \right\rangle$ values have a nonlinear dependence on transport stage (Figure 4b). We found that $\left\langle \overline{D_{st}} \right\rangle / h$ ranged from 0.062 to 0.14 across experiments, with the minimum and maximum $\left\langle \overline{D_{st}} \right\rangle / h$ values corresponding with threshold-of-motion ($\frac{\tau^*}{\tau_c^*}$ = 5.5) and bedload-dominated transport conditions ($\frac{\tau^*}{\tau_c^*}$ = 13.3). Low values of $\left\langle \overline{D_{st}} \right\rangle / h$ were recorded during threshold-of-motion transport conditions

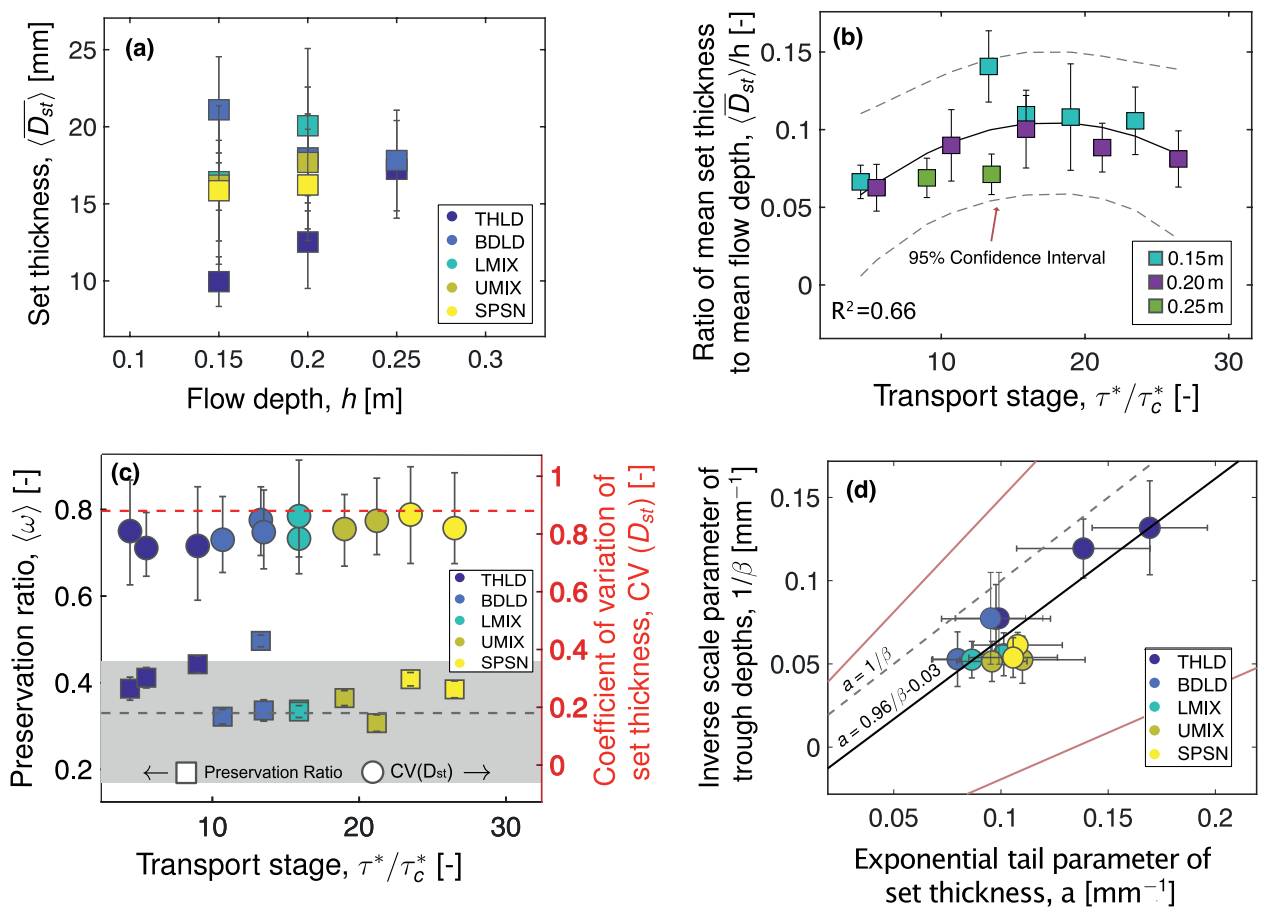

Figure 4. (a) The functional dependence of measured set thickness on flow depth. The error bars denote the standard deviation. (b) The functional dependence of mean set thickness normalized by flow depth on transport stage. The solid and dashed line indicate the best-fitting parabolic function and its 95% confidence intervals. Error bars indicate standard deviation. (c) Preservation ratio (left y-axis) and the coefficient of variation of set thickness (right y-axis) at various transport stages. Gray area denotes the empirically derived preservation ratio often used for paleohydraulic reconstruction (Leclair, 2002). The dashed red line denotes the theoretical expectation of $CV\ (D_{st}) = 0.88$ (Paola & Borgman, 1991). (d) Inverse of the scale parameter of the trough depths as a function of the exponential tail parameter of the set thickness distribution (Equation 3). The dashed line is the theoretical expectation of Paola and Borgman (1991). The markers and error bars in (c and d) denote the spatial averages of the quantities and the standard deviation computed across the 32 longitudinal transects in each experiment.

when the bed was covered with ripples/small dunes and during suspension-dominated transport conditions when dunes were nearly washed out. Higher values of $\left\langle \overline{D_{st}} \right\rangle / h$ corresponded with bedload-dominated and mixed-load conditions when the bed was characterized by large dunes. The parabolic dependence of $\left\langle \overline{H} \right\rangle$ and $\left\langle \overline{H_t} \right\rangle$ on transport stage translated into the preserved deposits, where the dependence of $\left\langle \overline{D_{st}} \right\rangle / h$ on τ^*/τ_c^* was best described by a parabolic function ($R^2 = 0.66$), and $\left\langle \overline{D_{st}} \right\rangle / h$ was maximized during intermediate transport stages (Figure 4b). Results indicate that 66% of the variability in preserved mean set thickness across experiments is explained by the variations in transport stage.

The preserved set thickness is consistent with the expectations of the variability-dominated preservation model across all experiments. The $\langle CV\ (D_{st}) \rangle$ ranged from 0.75 to 0.88 (Figure 4c), consistent with theory and the empirical range of 0.88 ± 0.30 proposed by Bridge (1997). Moreover, Equation 3 described the set thickness distribution for all experiments (Figures 3d–3f and S4 in Supporting Information S1). The scale parameter of the trough scour depth distribution is related to the parameter a of the theoretical set thickness distribution by $\beta = 1/a$ for all experiments. The best fitting regression line between a and $1/\beta$ across all experiments has a slope of 0.96 ± 0.40 (Figure 4d). Finally, we found that $\langle \omega \rangle$ ranged from 0.3 to 0.5, consistent with the empirical bounds of 0.17–0.45 proposed by Leclair (2002) (Figure 4c).

4. Discussion

The preserved set thickness is primarily controlled by the formative sediment transport conditions (Figure 4b). Our analyses revealed that the mean set thickness normalized by the formative flow depth has a parabolic dependence on transport stage. However, preserved set thickness displayed no apparent trend with flow depth across all experiments (Figure 4a). Preserved set thickness is greatest under bedload-dominated and lower mixed-load conditions for a given flow depth, similar to bedform heights and trough scour depths, which are also controlled by transport stage (Figures 3a and 3b). These results suggest that transport stage effects on bedform dimensions and set thickness, which are currently neglected, should be considered in paleo-flow depth reconstruction. In our experiments, bedform preservation ratio was consistent across transport stages and within the empirical range of 0.17–0.45 (Leclair, 2002, Figure 4c), indicating that $\left\langle \overline{H} \right\rangle = (2.9 \pm 0.7) \left\langle \overline{D_{\mathrm{st}}} \right\rangle$ can be used to reconstruct formative bedform heights from outcrop observations (Figure 4c; Leclair & Bridge, 2001). Moreover, empirical relation between mean bedform height and transport stage, derived from experimental and field data (R. W. Bradley and Venditti, 2019b),

$$\frac{\left\langle \overline{H} \right\rangle}{h} = -0.001\left(\frac{\tau^*}{\tau_c^*} - 17.69\right)^2 + 0.4169 \tag{4}$$

should be used to estimate paleo-flow depth. In this equation, τ_c^* can be estimated from measured D_{50} from outcrop observations, and making the normal-flow assumption and substituting $\tau^* = \frac{\rho_w h S}{(\rho_s - \rho_w) D_{50}}$ in Equation 4 results in two unknowns, namely, h and S. The paleoslope, S, can be constrained from established scaling relations that relate S to D_{50} and bankfull flow depth (Lynds et al., 2014; Trampush et al., 2014), which can be evaluated from observations of bar-scale stratigraphy (e.g., Alexander et al., 2020; Mohrig et al., 2000). Therefore, h is the only unknown in Equation 4 and can be solved for paleo-flow depth estimation.

Our results also indicate how the variability-dominated preservation model of Paola and Borgman (1991) describes the set thickness across all transport stages under steady-state conditions (Figure 4c). A two-parameter Gamma distribution describes the trough scour depths, similar to the bedform heights (e.g., Paola & Borgman, 1991) (Figure 3c), and the scale parameter of this distribution is inversely proportional to the parameter a that describes the set thickness distribution (Figure 4d; Paola & Borgman, 1991). Moreover, CV $(D_{\mathrm{st}}) \approx 0.88$ across all transport stages, indicating that deviations of CV(D_{st}) from the empirical range of 0.88 ± 0.30 (Bridge, 1997) can be attributed to the influence of flood variability and/or the coevolution of dunes in the presence of barforms (Ganti et al., 2020; Leary & Ganti, 2020; Lyster et al., 2022). These results suggest that the variability-dominated preservation model can be used to interpret outcrop observations so long as CV $(D_{\mathrm{st}}) \approx 0.88$ (Bridge, 1997; Leary & Ganti, 2020).

Flow-depth normalized trough scour depths also show a parabolic dependence on transport stage (Figure 3b). R. W. Bradley and Venditti (2019b) attributed the reduction in bedform heights at high transport stage to bedform flattening caused by suspension of sediment. In the experiments, trough depths accounted for more than half of the bedform heights (Figure S5 in Supporting Information S1), and the computed crest heights showed a weak dependence on transport stage ($R^2 = 0.26$; Figure S6 in Supporting Information S1). These observations indicate that the mechanics of scour in dunes are different from the processes of deposition. A significant amount of research has been dedicated to the mechanistic understanding of sediment accumulation in bedforms (e,g., Naqshband et al., 2017; Smith, 1970); however, the physical underpinnings of trough scouring are underexplored. Preservation of cross strata depends on the recurrence of scour, and future research should focus on the controls on recurrence of scours in bedform trains and their variation with flow and sediment transport conditions.

Finally, our work highlights that preserved cross strata encode information about the prevailing sediment transport conditions. Natural rivers experience a wide range of transport stages under flood hydrographs. For example, transport stage in the Fraser River varies from bedload-dominated conditions at low flows to suspension-dominated transport conditions during peak freshet flows (R. W. Bradley and Venditti, 2021). Our results demonstrate that such changes should be represented in the flow-depth-normalized set thickness. However, extracting this information requires the analysis of multiple hierarchical elements within the fluvial morphodynamic hierarchy (Ganti et al., 2020). The formative flow depths can be independently constrained from preserved bar clinoforms (e.g., Reesink, 2019; Mohrig et al., 2000), thus, enabling field estimation of $\left\langle \overline{D_{\mathrm{st}}} \right\rangle / h$, whilst transport stage can be

assessed from geometry and sorting of dune cross strata (Reesink and Bridge, 2009; Kleinhans, 2004). Trends in $\left\langle \overline{D_{st}} \right\rangle / h$ can then be used to quantify formative transport stages, where a lower $\left\langle \overline{D_{st}} \right\rangle / h$ value is expected for deposits corresponding to suspension-dominated conditions (peak flood) when compared to deposits constructed under bedload-dominated and lower-mixed load conditions (rising and falling limb of hydrograph). However, the parabolic relation between transport stage and $\left\langle \overline{D_{st}} \right\rangle / h$ implies non-unique solutions for formative transport stage (Figure 4c). Further investigation of set thickness across a range of flow depths and transport stages is essential for developing a robust functional relation between $\left\langle \overline{D_{st}} \right\rangle / h$ and transport stage that can inform the inversion of formative transport stage. Ultimately, the reconstruction of transport stage from preserved set thickness could form the basis for quantifying paleo-bed-material transport rates, thus opening up the potential to constrain paleo sediment fluxes.

5. Conclusions

We analyzed bedform evolution and preserved cross strata spanning a range of sediment transport conditions in an experimental flume to show that:

1. Transport stage exerts a primary control on preserved fluvial cross strata, and flow depth alone is a poor indicator of preserved set thickness.
2. The bedform trough depths normalized by the flow depth show a parabolic dependence on transport stage, similar to bedform heights, with the deepest scours occurring during bedload-dominated and mixed-load conditions.
3. The preserved set thickness normalized by the formative flow depth also displays a parabolic dependence on transport stage with maximum preserved set thickness occurring under bedload-dominated and mixed-load conditions.

Our findings highlight the need to incorporate transport stage effects on bedform dimensions in paleohydraulic reconstructions, and it provides a framework for assessing the prevailing sediment transport conditions from ancient deposits that may aid in the reconstruction of paleo-sediment transport rates of rivers.

Data Availability Statement

Data sets used in this research are publicly available at https://doi.org/10.25314/20c155da-4fcb-4a3f-9672-f02f8e2e33be. These data were previously reported in R. W. Bradley and Venditti (2019b).

Acknowledgments
This work was supported by the National Science Foundation EAR 1935669 grant and the donors of the American Chemical Society Petroleum Research Fund to Ganti, and the University of California Chancellor's Graduate Student Fellowship to Das. We thank P. Myrow and an anonymous reviewer for constructive comments on a previous draft.

References

Alexander, J. S., McElroy, B. J., Huzurbazar, S., & Murr, M. L. (2020). Elevation gaps in fluvial sandbar deposition and their implications for paleodepth estimation. *Geology*, *48*(7), 718–722. https://doi.org/10.1130/g47521.1

Allen, J. R. L. (1963a). The classification of cross-stratified units with notes on their origin. *Sedimentology*, *2*, 93–114. https://doi.org/10.1111/j.1365-3091.1963.tb01204.x

Allen, J. R. L. (1963b). Asymmetrical ripple marks and the origin of water-laid cosets of cross-strata. *Lpool Machr. Geological Journal*, *3*, 187–236.

Allen, J. R. L. (1970). A quantitative model of climbing ripples and their cross-laminated deposits. *Sedimentology*, *14*, 5–26. https://doi.org/10.1111/j.1365-3091.1970.tb00179.x

Allen, J. R. L. (1973). Features of cross-stratified units due to random and other changes in bed forms. *Sedimentology*, *20*, 189–202. https://doi.org/10.1111/j.1365-3091.1973.tb02044.x

Allen, J. R. L. (1982). Developments in sedimentology, sedimentary structures, their character and physical basis (Vol. 2). 30B.

Best, J., & Fielding, C. R. (2019). Describing fluvial systems: Linking processes to deposits and stratigraphy. *Geological Society, London, Special Publications*, *488*(1), 152–166. https://doi.org/10.1144/sp488-2019-056

Bhattacharya, J. P., & Tye, R. S. (2004). AAPG studies in geology No. 50: The Ferron Sandstone—Overview and reservoir analog) Chapter 2: Searching for modern Ferron analogs and application to Subsurface interpretation.

Bradley, R. (2018). *Transport scaling of Dunes in shallow flows*. Federated Research Data Repository.

Bradley, R. W., & Venditti, J. G. (2017). Reevaluating dune scaling relations. *Earth-Science Reviews*, *165*, 356–376. https://doi.org/10.1016/j.earscirev.2016.11.004

Bradley, R. W., & Venditti, J. G. (2019a). The growth of dunes in rivers. *Journal of Geophysical Research: Earth Surface*, *124*, 548–566. https://doi.org/10.1029/2018jf004835

Bradley, R. W., & Venditti, J. G. (2019b). Transport scaling of dune dimensions in shallow flows. *Journal of Geophysical Research: Earth Surface*, *124*, 526–547. https://doi.org/10.1029/2018jf004832

Bradley, R. W., & Venditti, J. G. (2021). Mechanisms of dune growth and decay in rivers. *Geophysical Research Letters*, *48*(20), e2021GL094572. https://doi.org/10.1029/2021gl094572

Bridge, J. S. (1997). Thickness of sets of cross strata and planar strata as a function of formative bed-wave geometry and migration, and aggradation rate. *Geology*, *25*(11), 971–974. https://doi.org/10.1130/0091-7613(1997)025<0971:tosocs>2.3.co;2
Bridge, J. S. (2003). *Rivers and floodplains: Forms, processes, and sedimentary record*. John Wiley & Sons.
Bridge, J. S., & Best, J. L. (1997). Preservation of planar laminae due to migration of low-relief bad waves over aggrading upper-stage plane beds: Comparison of experimental data with theory. *Sedimentology*, *44*, 253–262. https://doi.org/10.1111/j.1365-3091.1997.tb01523.x
Bridge, J. S., & Tye, R. S. (2000). Interpreting the dimension of ancient channel bars, channels, and channel belts from wireline-logs and cores. *AAPG Bulletin*, *84*, 1205–1228.
Edgar, L. A., Gupta, S., Rubin, D. M., Lewis, K. W., Kocurek, G. A., & Anderson, R. B. (2018). Shaler: In situ analysis of a fluvial sedimentary deposit on Mars. *Sedimentology*, *65*(1), 96–122. https://doi.org/10.1111/sed.12370
Ganti, V., Hajek, E. A., Leary, K., Straub, K. M., & Paola, C. (2020). Morphodynamic hierarchy and the fabric of the sedimentary record. *Geophysical Research Letters*, *47*(14), e2020GL087921. https://doi.org/10.1029/2020gl087921
Ganti, V., Paola, C., & Foufoula-Georgiou, E. (2013). Kinematic controls on the geometry of the preserved cross sets. *Journal of Geophysical Research: Earth Surface*, *118*, 1296–1307. https://doi.org/10.1002/jgrf.20094
Ganti, V., Whittaker, A. C., Lamb, M. P., & Fischer, W. W. (2019). Low-gradient, single-threaded rivers prior to greening of the continents. *Proceedings of the National Academy of Sciences*, *116*(24), 11652–11657. https://doi.org/10.1073/pnas.1901642116
Hu, H., Yang, Z., Yin, D., Cheng, H., & Parsons, D. R. (2021). Hydrodynamics over low-angle dunes at the tidal current limit of the Changjiang Estuary. *Estuarine, Coastal and Shelf Science*, *253*, 107298. https://doi.org/10.1016/j.ecss.2021.107298
Jerolmack, D. J., & Mohrig, D. (2005). Frozen dynamics of migrating bedforms. *Geology*, *33*(1), 57–60. https://doi.org/10.1130/g20897.1
Kleinhans, M. G. (2004). Sorting in grain flows at the lee side of dunes. *Earth-Science Reviews*, *65*(1–2), 75–102. https://doi.org/10.1016/s0012-8252(03)00081-3
Leary, K. C., & Ganti, V. (2020). Preserved fluvial cross strata record bedform disequilibrium dynamics. *Geophysical Research Letters*, *47*(2), e2019GL085910. https://doi.org/10.1029/2019gl085910
Leclair, S. F. (2002). Preservation of cross-strata due to the migration of subaqueous dunes: An experimental investigation. *Sedimentology*, *49*, 1157–1180. https://doi.org/10.1046/j.1365-3091.2002.00482.x
Leclair, S. F., & Bridge, J. S. (2001). Quantitative interpretation of sedimentary structures formed by river dunes. *Journal of Sedimentary Research*, *71*, 713–716. https://doi.org/10.1306/2dc40962-0e47-11d7-8643000102c1865d
Leclair, S. F., Bridge, J. S., & Wang, F. (1997). Preservation of cross-strata due to migration of subaqueous dunes over aggrading and non-aggrading beds: Comparison of experimental data with theory. *Geoscience Canada*, *24*, 55–66.
Lee, J., Musa, M., & Guala, M. (2021). Scale-dependent bedform migration and deformation in the physical and spectral domains. *Journal of Geophysical Research: Earth Surface*, *126*(5), e2020JF005811. https://doi.org/10.1029/2020jf005811
Lynds, R. M., Mohrig, D., Hajek, E. A., & Heller, P. L. (2014). Paleoslope reconstruction in sandy suspended-load-dominant rivers. *Journal of Sedimentary Research*, *84*(10), 825–836. https://doi.org/10.2110/jsr.2014.60
Lyster, S. J., Whittaker, A. C., Hajek, E. A., & Ganti, V. (2022). Field evidence for disequilibrium dynamics in preserved fluvial cross-strata: A record of discharge variability or morphodynamic hierarchy? *Earth and Planetary Science Letters*, *579*, 117355. https://doi.org/10.1016/j.epsl.2021.117355
Mahon, R. C., & McElroy, B. (2018). Indirect estimation of bedload flux from modern sand-bed rivers and ancient fluvial strata. *Geology*, *46*(7), 579–582. https://doi.org/10.1130/g40161.1
McElroy, B., & Mohrig, D. (2009). Nature of deformation of sandy bed forms. *Journal of Geophysical Research*, *114*, F00A04. https://doi.org/10.1029/2008jf001220
Mohrig, D., Heller, P. L., Paola, C., & Lyons, W. J. (2000). Interpreting avulsion process from ancient alluvial sequences: Guadalope-Matarranya system (northern Spain) and Wasatch Formation (Western Colorado). *The Geological Society of America Bulletin*, *112*(12), 1787–1803. https://doi.org/10.1130/0016-7606(2000)112<1787:iapfaa>2.0.co;2
Naqshband, S., Hoitink, A. J. F., McElroy, B., Hurther, D., & Hulscher, S. J. (2017). A sharp view on river dune transition to upper stage plane bed. *Geophysical Research Letters*, *44*(22), 11–437. https://doi.org/10.1002/2017gl075906
Paola, C., & Borgman, L. (1991). Reconstructing random topography from preserved stratification. *Sedimentology*, *38*, 553–565. https://doi.org/10.1111/j.1365-3091.1991.tb01008.x
Paola, C., Ganti, V., Mohrig, D., Runkel, A. C., & Straub, K. M. (2018). Time not our time: Physical controls on the preservation and measurement of geologic time. *Annual Review of Earth and Planetary Sciences*, *46*, 409–438. https://doi.org/10.1146/annurev-earth-082517-010129
Reesink, A. J. H. (2019). Interpretation of cross strata formed by unit bars. *Fluvial Meanders and Their Sedimentary Products in the Rock Record*, 173–200. https://doi.org/10.1002/9781119424437.ch7
Reesink, A. J. H., & Bridge, J. S. (2009). Influence of bedform superimposition and flow unsteadiness on the formation of cross strata in dunes and unit bars—Part 2, further experiments. *Sedimentary Geology*, *222*(3–4), 274–300. https://doi.org/10.1016/j.sedgeo.2009.09.014
Reesink, A. J. H., Van den Berg, J. H., Parsons, D. R., Amsler, M. L., Best, J. L., Hardy, R. J., et al. (2015). Extremes in dune preservation: Controls on the completeness of fluvial deposits. *Earth-Science Reviews*, *150*, 652–665. https://doi.org/10.1016/j.earscirev.2015.09.008
Rubin, D. M. (1987). *Cross-bedding, bedforms, and Paleocurrents: Concepts in sedimentology and Paleontology* (Vol. 1). SEPM.
Rubin, D. M., & Hunter, R. E. (1982). Bedform climbing in theory and nature. *Sedimentology*, *29*, 121–138. https://doi.org/10.1111/j.1365-3091.1982.tb01714.x
Shields, A. (1936). *Anwendung der Aehnlichkeitsmechanik und der Turbulenzforschung auf die Geschiebebewegung*, PhD Thesis Technical University.
Smith, J. D. (1970). Stability of a sand bed subjected to a shear flow of low Froude number. *Journal of Geophysical Research*, *75*(30), 5928–5940. https://doi.org/10.1029/jc075i030p05928
Sorby, H. C. (1859). On the structure produced by the currents during the deposition of stratified rocks. *GEOLOG*, *2*, 137–147. https://doi.org/10.1017/s1359465600021122
Storms, J. E. A., Dam, R. L. V., & Leclair, S. F. (1999). Preservation of cross-strata due to migration of current ripples over aggrading and non-aggrading beds: Comparison of experimental data with theory. *Sedimentology*, *46*, 189–200. https://doi.org/10.1046/j.1365-3091.1999.00212.x
Trampush, S. M., Huzurbazar, S., & McElroy, B. (2014). Empirical assessment of theory for bankfull characteristics of alluvial channels. *Water Resources Research*, *50*(12), 9211–9220. https://doi.org/10.1002/2014wr015597

Venditti, J. G., Lin, C. Y. M., & Kazemi, M. (2016). Variability in bedform morphology and kinematics with transport stage. *Sedimentology*, *63*(4), 1017–1040. https://doi.org/10.1111/sed.12247

Yalin, M. S. (1964). Geometrical properties of sand waves. *Journal of Hydraulic Engineering*, *90*, 105–119. https://doi.org/10.1061/jyceaj.0001097

References From the Supporting Information

Van der Mark, C. F., & Blom, A. (2007). *A new and widely applicable bedform tracking tool*. University of Twente.